

THE MAJORITY OF COMPACT MASSIVE GALAXIES AT $Z \sim 2$ ARE DISK DOMINATEDARJEN VAN DER WEL¹, HANS-WALTER RIX¹, STIJN WUYTS², ELIZABETH J. MCGRATH³, ANTON M. KOEKEMOER⁴, ERIC F. BELL⁵, BRADFORD P. HOLDEN³, ADAY R. ROBAINA⁶, DANIEL H. MCINTOSH⁷*The Astrophysical Journal, submitted*

ABSTRACT

We investigate the stellar structure of massive, quiescent galaxies at $z \sim 2$, based on *Hubble Space Telescope*/WFC3 imaging from the Early Release Science program. Our sample of 14 galaxies has stellar masses of $M_* > 10^{10.8} M_\odot$ and photometric redshifts of $1.5 < z < 2.5$. In agreement with previous work, their half-light radii are < 2 kpc, much smaller than equally massive galaxies in the present-day universe. A significant subset of the sample appears highly flattened in projection, which implies, considering viewing angle statistics, that a significant fraction of the galaxies in our sample have pronounced disks. This is corroborated by two-dimensional surface brightness profile fits. We estimate that $65\% \pm 15\%$ of the population of massive, quiescent $z \sim 2$ galaxies are disk-dominated. The median disk scale length is 1.5 kpc, substantially smaller than the disks of equally massive galaxies in the present-day universe. Our results provide strong observational evidence that the much-discussed ultra-dense high-redshift galaxies should generally be thought of as disk-like stellar systems with the majority of stars formed from gas that had time to settle into a disk.

1. INTRODUCTION

Structural evolution in the population of non-starforming (quiescent) galaxies has been observed and extensively discussed over the past few years. Such evolution has become an important ingredient in our description of evolutionary processes, and is used to constrain the theoretical framework for the formation of massive galaxies. The small sizes ($R_{\text{eff}} < 2$ kpc) of massive ($M \sim 10^{11} M_\odot$) quiescent galaxies at $z \sim 2$ have received particular attention, both in terms of explaining their formation and their subsequent evolution (e.g., Trujillo et al. 2004; Daddi et al. 2005; Papovich et al. 2005; Khochfar & Silk 2006; Trujillo et al. 2006b; Zirm 2007; Toft et al. 2007; van Dokkum et al. 2008; van der Wel et al. 2008; McGrath et al. 2008; Buitrago et al. 2008; Damjanov et al. 2009; van der Wel et al. 2009a; Saracco et al. 2009; Hopkins et al. 2009; van Dokkum et al. 2010; Cassata et al. 2010; Mancini et al. 2010; Szomoru et al. 2010).

The structural properties and surface brightness profiles of these compact, massive $z \sim 2$ galaxies, beyond their small sizes, can help us understand the formation scenario for these remarkable objects and their subsequent evolution: to produce such compact stellar systems, highly dissipative formation mechanisms have been proposed (e.g., Hopkins et al. 2009; Wuyts et al. 2010).

Although it is not clear whether stars have time to settle into a disk in such a scenario, this may imply that these objects should be rotating. On the other hand, given their high stellar masses, clustering properties (e.g., Quadri et al. 2007; Hartley et al. 2010), and number densities (e.g., van Dokkum et al. 2010), these objects must evolve into very massive, large, pressure-supported, bulge-dominated galaxies in the present-day universe.

In this paper we explore the internal structures and surface brightness profiles of massive, quiescent galaxies at $z \sim 2$, utilizing *Hubble Space Telescope* (*HST*)/WFC3 imaging, taken as part of the Early Release Science (ERS) program. We show that these galaxies are predominantly disk-like and describe the differences with their likely present-day descendants. From this, a consistent narrative emerges in which highly dissipative events produce compact, disk-dominated stellar systems, which subsequently experience a series of merger events, simultaneously explaining the growth in size and mass, and the lack of prominent disks in their descendants.

2. SAMPLE SELECTION AND DATA DESCRIPTION

FIREWORKS (Wuyts et al. 2008) provides a multi-wavelength catalog, from ground-based *U* band to *Spitzer* 24 μ m, and photometric redshifts. Stellar masses are derived for all sources with a minimum signal-to-noise ratio in the *K* band of 5, and photometric data points from at least four other bands. Following the procedure outlined by Marchesini et al. (2009), stellar-mass-to-light ratios are estimated from modeling the spectral energy distribution with the Bruzual & Charlot (2003) stellar population synthesis model for solar metallicity and exponentially declining star formation rates. We adopt the Kroupa (2001) stellar initial mass function, and the assumed cosmology is $(\Omega_M, \Omega_\Lambda, h) = (0.3, 0.7, 0.7)$.

We select all galaxies with photometric redshifts $1.5 < z < 2.5$ and stellar masses $M > 10^{10.8} M_\odot$, at which the catalog is complete. Based on their rest-frame $r - z$ and $u - r$ colors we select those galaxies which are quiescent

¹ Max-Planck Institut für Astronomie, Königstuhl 17, D-69117, Heidelberg, Germany; vdwel@mpia.de

² Max-Planck-Institut für Extraterrestrische Physik, Giessenbachstrasse, D-85748 Garching, Germany

³ University of California Observatories/Lick Observatory, University of California, Santa Cruz, CA 95064, USA

⁴ Space Telescope Science Institute, 3700 San Martin Drive, Baltimore, MD 21218, USA

⁵ Department of Astronomy, University of Michigan, 500 Church Street, Ann Arbor, Michigan, 48109, USA

⁶ Institut de Ciències del Cosmos, University of Barcelona, Marté i Franquès, 1 E-08028, Barcelona, Spain

⁷ Department of Physics, University of Missouri-Kansas City, Kansas City, MO 64110, USA

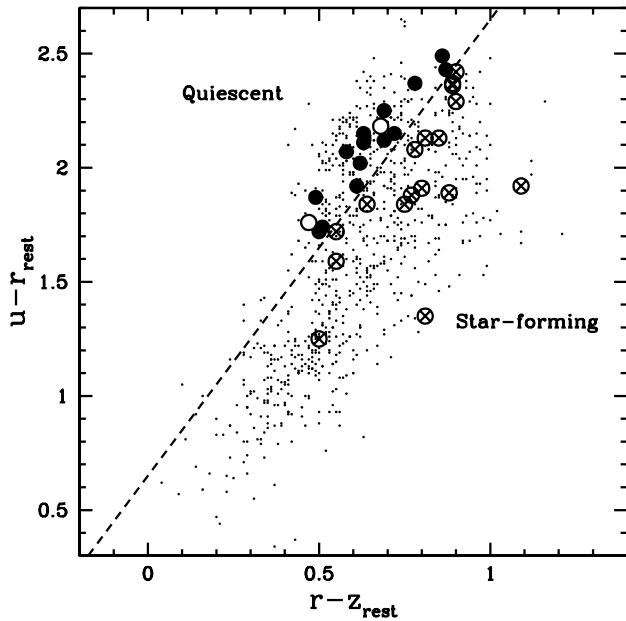


Figure 1. Rest-frame $u - r$ vs. $r - z$ color for galaxies drawn from the FIREWORKS catalog (Wuyts et al. 2008). Dots represent galaxies in the redshift range $1 < z < 2$ and with stellar masses $M > 10^{10} M_{\odot}$, shown to demonstrate that galaxies separate into a star-forming sequence (below the dashed line), along which the extinction increases toward the top right, and a quiescent sequence (see Williams et al. 2009, for a more clearly defined bi-modal distribution). Large symbols represent galaxies with stellar masses $M > 10^{10.8} M_{\odot}$ in our redshift range of interest ($1.5 < z < 2.5$) and within the *HST*/WFC3 ERS mosaic. We select the 14 objects (indicated by filled circles) upward from the dashed line as our sample of massive, quiescent $z \sim 2$ galaxies. The objects indicated with open circles with crosses are considered star forming and not included in our sample. Two galaxies, indicated by open circles, that satisfy the color-criteria are excluded from the analysis (see the text).

(see Figure 1): galaxies with blue $u - r$ colors are excluded on the basis of the directly observed young stellar populations; galaxies with red $r - z$ colors are excluded based on the red color long-ward of the 4000Å/Balmer break, indicative of reddening by dust. Such a technique was first used by Wuyts et al. (2007) and, subsequently, for a much larger sample by Williams et al. (2009). Whereas these authors use the $U - V$ and $V - J$ color combination, our $u - r$ and $r - z$ color combination is essentially equally effective (B. P. Holden et al. , 2011, in preparation).

Sixteen of these galaxies are in the Chandra Deep Field-South WFC3/ERS2 region (Windhorst et al. 2010), for which an independent reduction of the 10 pointings (5000s total) into an F160W mosaic was carried out by A. M. Koekemoer et al. (2011, in preparation) using Multidrizzle (Koekemoer et al. 2002).

Two of the 16 galaxies are excluded from further analysis: one is a merger with strong tidal features; the other is located at a small projected distance from a very bright foreground galaxy, which precludes accurate photometry and analysis.

We subject the images of the 14 remaining galaxies to the Lucy-Robertson deconvolution algorithm (“lucy” in IRAF), iterating 16 times, using a point spread function (PSF) created with TinyTim (Krist 1995), taking into account the dither pattern of the observations and the

Multidrizzle data processing. The reconstruction brings out small-scale (~ 800 pc), high surface brightness features.

We show the original and deconvolved images in Figure 2. Structural parameters are inferred from fitting single-component Sersic models with GALFIT (Peng et al. 2002) to the original images, using the same PSF as described above. All 14 galaxies, which have a median stellar mass of $10^{11.1} M_{\odot}$, have circularized half-light radii smaller than 2 kpc (the median is 1.2 kpc), in agreement with previous studies, a median Sersic index of 2.5, and a median axis ratio of 0.67, almost identical to that of the sample of van Dokkum et al. (2008).

We also determine, in the same manner, the structural parameters of the star-forming galaxies, that is, those below the dashed line in Figure 1. Their median Sersic index and axis ratio are $n = 1.5$ and $b/a = 0.53$, respectively. Their sizes vary with distance to the dashed line in Figure 1: those close to the line have sizes 1.5–2 kpc, comparable to the galaxies in our quiescent sample, while those far from the line are larger (4–5 kpc). This implies that our results do not depend on the exact criterion for quiescence.

3. THE DISK-LIKE NATURE OF MASSIVE $Z = 2$ GALAXIES

A significant fraction of the galaxies shown in Figure 2 are strongly flattened in projection – the galaxies 2, 7, 8, 11, and 12 have best-fitting axis ratios $b/a \lesssim 0.5$, indicative of a disk-like structure. Viewed more face-on, this would be difficult to recognize. Assuming approximately random viewing angles, this implies that a significant fraction – at face value a majority – of massive, quiescent $z \sim 2$ are disk-dominated.

To follow up on the evidence based on the axis ratio distribution, we examine the disk-like nature of the individual galaxies by performing two-component fits with GALFIT on the original images, using the same PSF as before. The positions of the two components are kept fixed at the position of the one-component fit, and the Sersic index is fixed at $n = 1$ for the disk-like component. All other parameters are left free. In Figure 3 we show 4 examples of the two-component fits and point out the similarity between the two-component model fits and the deconvolved images shown in Figure 2.

We explore the uncertainty in the two-component fits by artificially doubling the rms in the background by adding Gaussian noise, and by using two different PSF models: a PSF that is constructed from bright stars in the same mosaic, and a simpler TinyTim-based PSF. These alternative PSFs are known to be a less accurate representation of the true PSF than our preferred, default PSF.

For four out of 14 galaxies (nos. 2, 10, 11, 12) we reproduce the disk-dominated two-component fits regardless of the adopted PSF model and the artificially increased noise level. For another three galaxies (nos. 4, 5, 8) with disk-dominated two-component fits from our preferred PSF and original noise level, the fitting parameters change with PSF choice and noise level to the extent that we consider the evidence for the disk-dominated nature of these objects as tentative.

For these 4+3 galaxies either the χ^2 value of the two-component fit is significantly lower than that of the one-component fit, or the one-component fit is disk-like itself

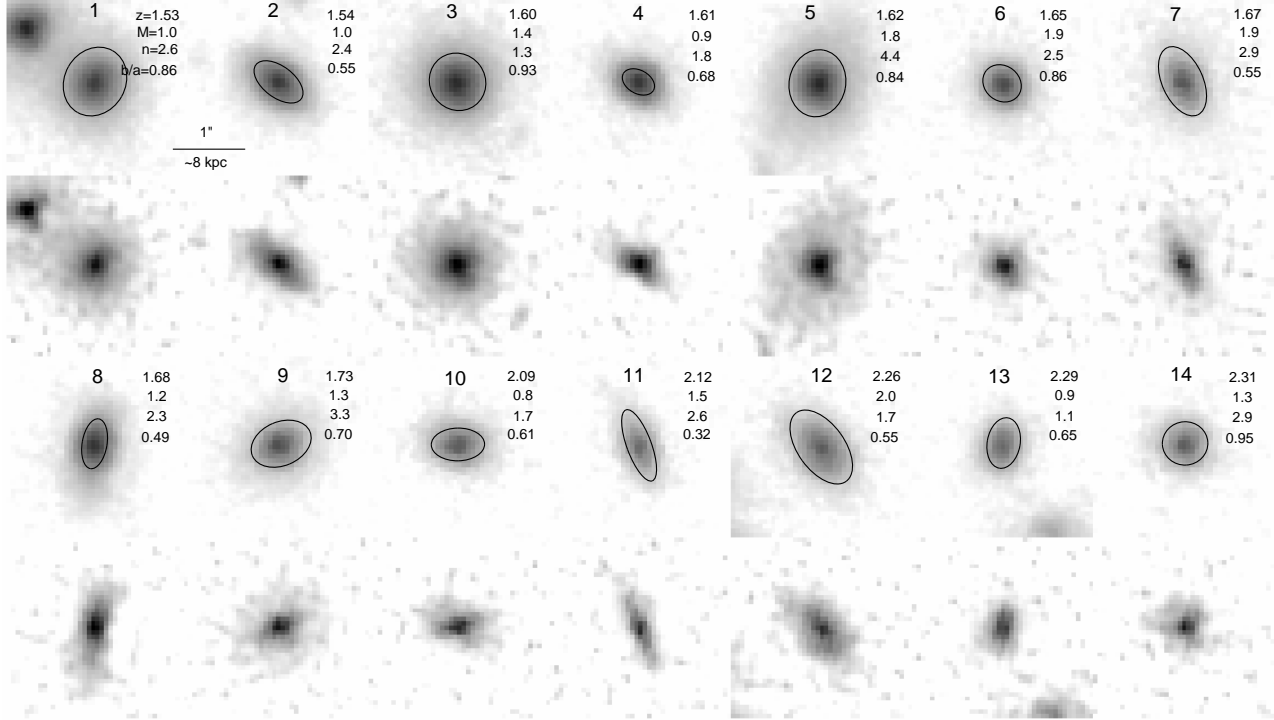


Figure 2. *HST/WFC3* F160W imaging of our sample of massive, quiescent $z \sim 2$ galaxies (all with $H_{\text{F160W}} < 23$). The deconvolved images are shown directly below the original images. Photometric redshifts, stellar masses (in units of $10^{11} M_{\odot}$), Sersic indices, and axis ratios from one-component profile fits, as well as the scale of the images, are indicated. Ellipses indicate best-fitting axis ratios and sizes from GALFIT – the area of the ellipse corresponds to that of a circle with a radius that is twice the circularized half-light radius. All galaxies are clearly resolved and many are flattened in projection, indicative of a disk-like stellar structure.

(with Sersic index $n \lesssim 2$). For the other 7 galaxies the fitting could not directly ascertain whether they are disk-dominated.

To estimate the disk-dominated fraction among massive, quiescent $z \sim 2$ galaxies, we combine the results from the quantitative two-component fits with the visual impression reflected in Figure 2 (mostly flatness), which are independent of each other. All four galaxies with robust disk-dominated two-component fits are flat in projection (with $b/a \leq 0.6$). We assign those objects weights of 0.9 (90% probability that these galaxies are, in fact, disk-dominated). We assign weight 0.7 to those 3 galaxies with more tentative quantitative evidence. These weights/probabilities should not be considered precise and quantitative, but serve as a proxy for our level of confidence that these galaxies are disk-dominated.

If we conservatively assume that none of the other seven galaxies are disk dominated (i.e., they have weight 0), then we infer that $40\% \pm 15\%$ of the population of massive, quiescent $z \sim 2$ galaxies is disk dominated. This number and its uncertainty include the weights as specified above and the uncertainty due to the small sample size.

However, some of the 7 non-classified galaxies, for example, 7 and 13, have small axis ratios. Therefore, it is not reasonable to interpret the lack of quantitative evidence for dominant disks as evidence for the absence of such disks. If we assign weight 0.5 to those objects, we infer that $65\% \pm 15\%$ of the population of massive, quiescent $z \sim 2$ galaxies is disk-dominated.

We have not attempted a more formal inversion of

the intrinsic axis ratios as our sample is too small to de-project the observed axis ratio distribution without making overly restrictive assumptions about the underlying intrinsic axis ratio distribution. Qualitatively, however, the general flatness of the galaxies in our sample is consistent with a population with disks of finite intrinsic thickness (~ 0.25). We stress that simply considering the observation that 5 out of 14 galaxies have axis ratios $b/a \leq 0.55$ leads to a similar conclusion that $\sim 50\% - 100\%$ of the galaxies in the sample must be intrinsically thin, that is, disk-like: face-on counterparts of the observed edge-on disk-like galaxies must exist as well.

We note that while very prolate systems can also lead to frequent small projected axis ratios, we consider this possibility unlikely: the absence of very prolate self-gravitating systems at lower redshifts suggests that nature does not produce such objects, and this should be independent of cosmic time.

Based on examining the also available F125W and F098N imaging of our sample, we are confident that our inferences from the light profiles directly translate into information about the stellar mass distribution. The F125W and F160W images (roughly corresponding to B and V in the rest frame) are very similar in appearance, and all galaxies are much fainter in the bluer F098N passband (rest-frame U). We show color images for four disk-dominated galaxies in Figure 3; these illustrate that strong color gradients are absent, which implies that the disks are not strongly star forming.⁸ In other words,

⁸ None of these examples have $24\mu\text{m}$ counterparts that signify star formation rates in excess of $\sim 20 M_{\odot}\text{yr}^{-1}$, which is less than

the light distribution must be similar to the stellar mass distribution.

The major axis exponential scale length of the disks of the galaxies we consider as disk-dominated ranges from 1 to 4 kpc, with a median of 1.5 kpc; this is substantially smaller than the scale lengths of disks in similarly massive galaxies in the present-day universe, which is ~ 4 kpc ($\log(R_d/\text{kpc}) = 0.6 \pm 0.1$, where 0.1 is the 1σ scatter, Fathi et al. (2010); Fathi (2010)). The median scale length for our sample deviates by $\sim 3\sigma$, which implies that it is unlikely that most of these disk-like structures will survive up until the present day.

Several studies have before measured the size evolution of disk-like and bulge-like galaxies based on their Sersic indices (Trujillo et al. 2006b; Buitrago et al. 2008), but only for stellar mass selected samples that include star-forming galaxies. Stockton et al. (2006), McGrath et al. (2008), and Stockton et al. (2008) reported the existence of passive, massive galaxies at $z > 1.5$ with disk-like surface brightness profiles, showing that a mix of morphological properties exists among passive, high-redshift galaxies. However, the population of compact galaxies reported by, for example, Zirm (2007) and van Dokkum et al. (2008) have not been identified with disk-dominated morphologies, but are generally thought of as early-type, bulge-like structures. Although van Dokkum et al. (2008) mention the disk-like nature of some of the galaxies in their sample, they did not consider the implications for the overall population statistics.

Our findings suggest that the majority of compact, massive, quiescent $z \sim 2$ galaxies are disk-dominated, typically hosting stellar disks with scale radii that are several times smaller than present-day disks.

4. FORMATION AND EVOLUTION

The scale lengths of the stellar disks in quiescent $z \sim 2$ galaxies are, on average, ~ 3 times smaller than the scale lengths of similarly massive present-day stellar disks (see Section 3). This is consistent with the zeroth-order theoretical expectation: the size and angular momentum of a $z \sim 2$ dark matter halo are on average ~ 3 times smaller than those of a similarly massive present-day dark matter halo. The assumption here is that the correspondence between a disk and its halo in terms of relative mass, size, and angular momentum does not evolve (Mo et al. 1999). While these assumptions are obviously not strictly valid, it is still not unexpected that stellar disks are several times smaller at $z \sim 2$ than at the present. In addition, the global compactness of quiescent galaxies at $z \sim 2$ is further boosted by the presence of compact, central components – these galaxies are not pure disks.

Simulations of gas-rich mergers produce descendants that are broadly reminiscent of the observed galaxies, most particularly in the sense that these simulated merger remnants have substantial rotation, and must therefore be disk-like (Wuyts et al. 2010). Moreover, the simulations produce dense cores, and more extended outer parts. However, there are important quantitative differences. The merger remnants are entirely unlike exponential disks – they have very high Sersic indices, $n > 4$. This is the result of overly dominant central com-

the average past star formation rate for these galaxies, qualifying them as quiescent.

pact components. Gradual gas accretion to produce a disk, combined with the occasional (minor) merger event to produce a modest central component, may explain the described structural properties of quiescent $z \sim 2$ galaxies. Generally speaking, their formation mechanism must be sufficiently gentle and slow as to allow gas to settle onto a disk before converting into stars.

However, we note that the quiescent galaxies are not simply $z \sim 2$ star-forming galaxies of which the star formation rate has been reduced from $100 - 1000 M_{\odot} \text{ yr}^{-1}$ (Förster Schreiber et al. 2009) to $\lesssim 20 M_{\odot} \text{ yr}^{-1}$. Although massive star-forming galaxies at $z \sim 2$ are also disk-like in their structural parameters (see Section 3 and, e.g., Labb   et al. 2003; F  rster Schreiber et al. 2010) as well as in their dynamical properties (e.g., F  rster Schreiber et al. 2009; Genzel et al. 2010), their disks are substantially larger (with scale lengths of ~ 3 kpc) than the quiescent disks described here and only somewhat smaller than present-day disks. The explanation for this may be the age difference between the quiescent and star-forming galaxies: the star-forming galaxies are undergoing a major, possibly first, episode of significant growth, while the quiescent galaxies must have undergone such a phase at an earlier epoch, implying smaller sizes (see also Franx et al. 2008; van der Wel et al. 2009a). The correlation between color and size for star-forming galaxies (Section 2) is consistent with this picture.

Let us now consider the evolutionary path between the epoch of observation, $z \sim 2$, and the present day. In a hierarchical Λ CDM universe, the descendants of $\sim 10^{11} M_{\odot}$ $z \sim 2$ galaxies are super- L^* galaxies with masses $> (2 - 3) \times 10^{11} M_{\odot}$. This argument is bolstered by the observed clustering of massive $z \sim 2$ galaxies in comparison with the clustering properties of very massive galaxies in the present-day universe (Quadri et al. 2007; Hartley et al. 2010). A simple, model-independent argument to the same effect is that the comoving number density of $z \sim 2$ galaxies with stellar masses $\sim 10^{11} M_{\odot}$ is the same as that of present-day galaxies with stellar masses $\sim 3 \times 10^{11} M_{\odot}$ (van Dokkum et al. 2010). That is, these disk-like $z \sim 2$ galaxies are *not* progenitors of Milky Way type galaxies at the present day.

Thus, we have compact, disk-dominated galaxies at $z \sim 2$, the present-day descendants of which are 2 – 3 times more massive, are ~ 5 times larger in half-light radius, and almost never have prominent stellar disks (van der Wel et al. 2009b). Clearly, the structure of these galaxies has evolved dramatically over the past 10 Gyr. Growth in mass through merging by the relatively modest factor of two or three compares well with observed merger rates (e.g., Robaina et al. 2010) and model expectations (Hopkins et al. 2010). The expected merger trees consist of a mix of frequent minor mergers/accretion events and rare major mergers with low overall gas fractions ($\lesssim 2$ per galaxy since $z = 2$). The former are generally thought to provide the most efficient mechanism to explain size evolution (e.g., Bezanson et al. 2009; van der Wel et al. 2009a). Indeed, the gradual buildup of the outer parts associated with such accretion events has been observed (van Dokkum et al. 2010). To destroy a massive stellar disk, major merging is more efficient, although a sequence of many minor accretion events can have the same

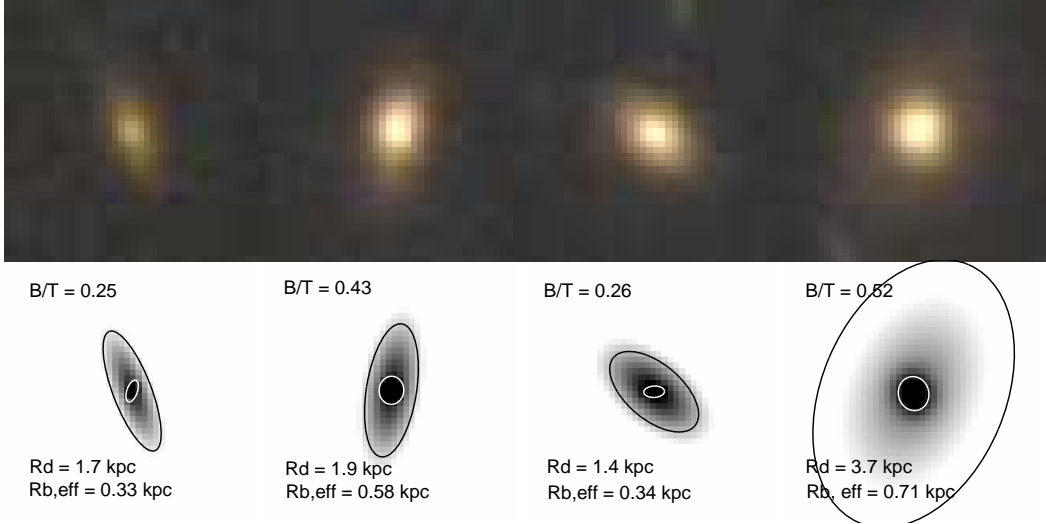


Figure 3. Top: F098N+F160W color composites for galaxies 11, 8, 2, and 5 from Figure 2, ordered by axis ratio. These four examples are chosen because of their flatness, with the exception of no. 5, which appears to have a compact bulge-like component surrounded by a more extended, disk-like component. There is no strong indications for color gradients, suggesting that the disk-components of these galaxies are not strongly star forming. Bottom: two-component model fits (without PSF smearing) for the same galaxies. The white and black ellipses indicate twice the size of the half-light ellipses for bulge-like and disk-like components, respectively. B/T is the ratio of the light in the model for the bulge-like component and the light of the models for the two components combined. “ R_d ” is the exponential scale length as measured along the major axis of the disk-like component, which we calculate by dividing the semimajor axis of the “half-light ellipse” by 1.6. “ $R_{b,eff}$ ” is the circularized half-light radius of the bulge-like component.

effect (Naab et al. 1999; Bournaud et al. 2007). Overall, a consistent narrative is emerging in which merging and accretion explain the growth in size and change in structure of massive, passive galaxies over time.

Further support for the direct link between the disk-like galaxies at $z \sim 2$ and the pressure-supported, massive elliptical galaxies in the present-day universe is provided by the comparable stellar densities of the $z \sim 2$ galaxies and the cores of present-day ellipticals (Bezanson et al. 2009; Hopkins et al. 2009; van Dokkum et al. 2010). Dynamical modeling of very massive nearby ellipticals has revealed that whereas the global rotation rate is small, the majority of the stars, even in the inner parts, are on disk-like orbits (see van den Bosch et al. 2008, for an example). This may be the archaeological remnant of the disk-like nature of its progenitors.

The authors thank the referee, Matthew Bershady, for helpful suggestions that helped improve the paper, and Kambiz Fathi for sharing his disk scale length measurements and comments on the manuscript.

REFERENCES

- Bezanson, R., van Dokkum, P. G., Tal, T., Marchesini, D., Kriek, M., Franx, M., & Coppi, P. 2009, ApJ, 697, 1290
 Bournaud, F., Jog, C. J., & Combes, F. 2007, A&A, 476, 1179
 Bruzual, G., & Charlot, S. 2003, MNRAS, 344, 1000
 Buitrago, F., Trujillo, I., Conselice, C. J., Bouwens, R. J., Dickinson, M., & Yan, H. 2008, ApJ, 687, L61
 Cassata, P. et al. 2010, ApJ, 714, L79
 Daddi, E. et al. 2005, ApJ, 626, 680
 Damjanov, I. et al. 2009, ApJ, 695, 101
 Fathi, K. 2010, ApJ, 722, L120
 Fathi, K., Allen, M., Boch, T., Hatziminaoglou, E., & Peletier, R. F. 2010, MNRAS, 406, 1595
 Förster Schreiber, N. M. et al. 2009, ApJ, 706, 1364
 Förster Schreiber, N. M., Shapley, A. E., Erb, D. K., Genzel, R., Steidel, C. C., Bouché, N., Cresci, G., Davies, R. 2010, ApJ, submitted, arXiv:1011.1507
 Franx, M., van Dokkum, P. G., Förster Schreiber, N. M., Wuyts, S., Labb  , I., & Toft, S. 2008, ApJ, 688, 770
 Genzel, R. et al. 2010, ApJ, submitted, arXiv:1011.5360
 Hartley, W. G. et al. 2010, MNRAS, 407, 1212
 Hopkins, P. F. et al. 2010, ApJ, 715, 202
 Hopkins, P. F., Hernquist, L., Cox, T. J., Keres, D., & Wuyts, S. 2009, ApJ, 691, 1424
 Koekemoer, A. M., Fruchter, A. S., Hook, R. N., & Hack, W. 2002, The 2002 HST Calibration Workshop : Hubble after the Installation of the ACS and the NICMOS Cooling System, 337
 Khochfar, S., & Silk, J. 2006, ApJ, 648, L21
 Krist, J. 1995, ASPC, 77, 349
 Kroupa, P. 2001, MNRAS, 322, 231
 Labb  , I. et al. 2003, ApJ, 591, L95
 Mancini, C. et al. 2010, MNRAS, 401, 933
 Marchesini, D., van Dokkum, P. G., Förster Schreiber, N. M., Franx, M., Labb  , I., & Wuyts, S. 2009, ApJ, 701, 1765
 McGrath, E. J., Stockton, A., Canalizo, G., Iye, M., & Maihara, T. 2008, ApJ, 682, 303
 Mo, H. J., Mao, S., & White, S. D. M. 1999, MNRAS, 304, 175
 Naab, T., Burkert, A., & Hernquist, L. 1999, ApJ, 523, L133
 Papovich, C., Dickinson, M., Giavalisco, M., Conselice, C. J., & Ferguson, H. C. 2005, ApJ, 631, 101
 Peng, C. Y., Ho, L. C., Impey, C. D., & Rix, H.-W. 2002, AJ, 124, 266
 Quadri, R. et al. 2007, ApJ, 654, 138
 Robaina, A. R., Bell, E. F., van der Wel, A., Somerville, R. S., Skelton, R. E., McIntosh, D. H., Meisenheimer, K., & Wolf, C. 2010, ApJ, 719, 844
 Saracco, P., Longhetti, M., & Andreon, S. 2009, MNRAS, 392, 718
 Stockton, A., McGrath, E., & Canalizo, G. 2006, ApJ, 650, 706
 Stockton, A., McGrath, E., Canalizo, G., Iye, M., & Maihara, T. 2008, ApJ, 672, 146
 Szomoru, D. et al. 2010, ApJ, 714, L244
 Toft, S. et al. 2007, ApJ, 671, 285
 Trujillo, I. et al. 2004, ApJ, 604, 521
 Trujillo, I. et al. 2006b, ApJ, 650, 18
 van den Bosch, R. C. E., van de Ven, G., Verolme, E. K., Cappellari, M., & de Zeeuw, P. T. 2008, MNRAS, 385, 647

- van der Wel, A., Bell, E. F., van den Bosch, F. C., Gallazzi, A., & Rix, H.-W. 2009a, *ApJ*, 698, 1232
- van der Wel, A., Holden, B. P., Zirm, A. W., Franx, M., Rettura, A., Illingworth, G. D., & Ford, H. C. 2008, *ApJ*, 688, 48
- van der Wel, A., Rix, H.-W., Holden, B. P., Bell, E. F., & Robaina, A. R. 2009b, *ApJ*, 706, L120
- van Dokkum, P. G. et al. 2008, *ApJ*, 677, L5
- van Dokkum, P. G. et al. 2010, *ApJ*, 709, 1018
- Williams, R. J., Quadri, R. F., Franx, M., van Dokkum, P., & Labb  , I. 2009, *ApJ*, 691, 1879
- Windhorst, R. A., et al. 2010, arXiv:1005.2776
- Wuyts, S. et al. 2010, *ApJ*, 722, 1666
- Wuyts, S. et al. 2007, *ApJ*, 655, 51
- Wuyts, S., Labb  , I., F  rster Schreiber, N. M., Franx, M., Rudnick, G., Brammer, G. B., & van Dokkum, P. G. 2008, *ApJ*, 682, 985, 2008
- Zirm, A. W. et al. 2007, *ApJ*, 656, 66